Solid Freeform Fabrication 2023: Proceedings of the 34th Annual International Solid Freeform Fabrication Symposium – An Additive Manufacturing Conference
Reviewed Paper

Fundamentals of Polymer Crystallization in Laser Powder Bed Fusion for New Material Screening

Camden A. Chatham[a], Samantha J. Talley[b]

[a]Advanced Engineering Division, Savannah River National Laboratory,
Savannah River Site, Aiken, 29808, SC, USA

[b]Materials Engineering, Kansas City National Security Campus,
14520 Botts Rd, Kansas City, 64147, MO, USA

Abstract

Although laser powder bed fusion (PBF/LB) was one of the first industrially viable additive manufacturing (AM) methods for end-use part production, polyamides remain grossly dominant at both the commercial- and research scale. The research community continues to develop and refine "rapid screening" methods for evaluating the suitability of new polymers for PBF/LB. The so-called "SLS Process Window," which is the difference between melting and crystallization temperature measured at 10 K min^{-1} as originally outlined in the patent literature, is perhaps the most often reported screening method. Although perhaps appropriate as part of a larger study, the simplistic guidelines put forth by the "SLS Process Window" are not sufficiently scientifically rigorous to understand how crystallization kinetics affects successful 3D printing. The common understanding of the SLS Process Window omits details from published theories of polymer crystallization. as evidenced by published assumptions and methods in PBF/LB process modeling papers. The authors explain polymer crystallization in the PBF/LB context and propose replacing the "process window" with crystallization halftime and physical gelation for new material screening. These measurements better represent behavior critical for ensuring a lengthy coexistence of solid powder and molten polymer affecting warp-free parts.

Introduction

In general, thermoplastic additive manufacturing (AM) can be divided into material extrusion (MEX) for amorphous polymers and laser powder bed fusion (PBF/LB) (originally commercialized as Selective Laser Sintering; SLS [1]) for semi-crystalline polymers. All thermoplastic manufacturing methods require in-depth understanding of the relationship between polymer viscosity, temperature, and pressure. For semi-crystalline polymers, this includes the first-order thermal transitions for melting and crystallization, which have a profound effect on viscosity. The rapid heating and cooling cycles arising from PBF/LB's distinctive laser scanning is a complex environment for melting and crystallization often considered to be quasi-isothermal by the modeling community [2]. Despite the complex temperature profiles, many investigations into adapting or evaluating the potential printability of polymers in PBF/LB hinge on the so-called "SLS Processing Window." Constructing the SLS Processing Window involves running a dynamic differential scanning calorimetry (DSC) experiment at either 10 or 20 °C min^{-1} and observing the degree of separation on the temperature axis between melting and crystallization behavior. Statements published in the literature regarding this technique indicate that (i) a wider window is

better [3, 4] and (ii) the observed separation of melting and crystallization behaviors *must* occur for successful printing [3, 5]. Other authors claim observing this behavior indicates that (iii) the scanned polymer remains molten throughout the entire build [6, 7, 8]. The authors believe that, although these statements originated from scientifically sound claims from the patent literature, the common use in published literature falls short of accurately describing polymer behavior in a manner consistent with the historic body of polymer crystallization literature. Failing to recognize the simplifications made in the patent literature is hindering the research community from developing and/or adapting new polymers for PBF/LB. In this paper, the authors present the original usage and merits of the PBF/LB Processing Window as a cursory first glance at understanding the relationship between viscosity, morphology, and temperature before highlighting the simplifications made for the sake of patent claims and expounding on the fundamentals of polymer crystallization applied to the PBF/LB context.

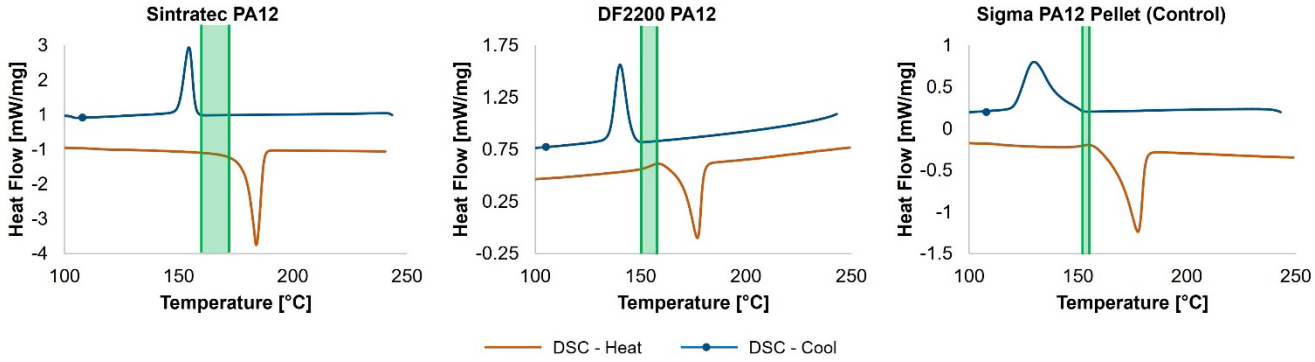

Figure 1: The oft reported "SLS Processing Window" overlay of DSC heating and cooling data collected at 10 °C min^{-1} for two AM-grade nylon-12 materials and a pellet nylon-12 control. Annotations highlight the separation between melting and crystallization behavior.

The Historical Use of the PBF/LB Processing Window

The technology known as "laser based polymer powder bed fusion (PBF/LB-P)" according to ASTM/ISO 52900-21 [9] was originally patented and commercialized as "Selective Laser Sintering (SLS)" by Carl Deckard and DTM Corporation [10, 1]. The method describes using a laser beam to selectively heat and fuse together powdered polymer in a layerwise manner to generate a 3D object. The so-called "SLS Process Window" originates from subsequent DTM Patent literature. Follow-on patents in 1994 and 1997 by DTM describe commonalities among materials that could be successfully printed by this method. [11, 12]. The patents describe either "non-overlapping" (1994) or "slightly overlapping" (1997) temperature regions for observed melting and crystallization behavior when the material is evaluated by a dynamic DSC experiment measured using a reasonable heating rate between 10-20 °C min^{-1}. The patents describe example successful materials being printable with as much as a 13 °C temperature overlap accounting for 6.2 % of the integrated area underneath the melting and crystallization curves. Conversely, negative examples of unsuccessfully printed materials are showing a 24 °C and 21 % overlap in melting and crystallization behavior [12]. The patent goes on to state that although this method is not a measurement of crystallization rate, it is related to crystallization rate.

The vague patent language has apparently influenced both the reported figures and the tone of discussion in the scientific literature. Interestingly, scientific articles often provide less discussion than the patents on the fundamental physics principles underlying the "sintering window." Some simply report the separation in melting and crystallization temperature without

mention of the rationale that this measurement is related to crystallization rate [13]. Others explicitly state that the observed separation of behavior is critical for successful printing [3, 5, 7] even though this is counter to the 1997 patent, which allows for small overlaps [12].

Bain's 2019 summary of the "so-called sintering window" asserts the intended goal of the measurement as demonstrating a slow crystallization rate to afford both thoroughly coalesced particles and no out-of-plane warping [14]. "Slow" is a vague and relative term that is not particularly helpful in PBF/LB material screening. "Slow" is not quantitative; one cannot know by this method only if it is "slow enough" for the PBF/LB context.

Warping is another aspect of DTM's patents that is rarely discussed in scientific literature. They make the claim outlining a critical minimum storage modulus for the polymer being printed that will not allow more than 50 μm of out of plane curling. Crystallization and its accompanying discrete reduction in specific volume is often cited as the major cause of out of plane warping leading to build failure; however, little discussion is given to the forces opposing warping including in review papers like those written by Bain [14] and Chatham, et al. [15].

Fundamentals of Polymer Crystallization

This section covers selected aspects of current understanding in the polymer science community of polymer melting and crystallization phenomena at a high level. References in this section are not explicitly tied to the PBF/LB or any manufacturing context. It is included to orient the reader around the wider wealth of research reported from studying polymer melting and crystallization.

Equilibrium melting and supercooling. The equilibrium melting temperature (T_m^0) is the temperature above which a given polymer will never form stable regions of crystallinity. It designates the threshold where melting and crystallization are in equilibrium for an extended-chain crystal (i.e., no folds in polymer chain conformation) [16]. It is often calculated based on Hoffman-Weeks theory extrapolating a linear fit of measure peak melting temperatures following complete crystallization at an independently determined isothermal crystallization temperature [17]. The difference between T_m^0 and each independently determined (i.e., set by the researcher) temperature is termed the "undercooling" or "supercooling." When PBF/LB - focused papers or patents employ the term "supercooling" they are more often referring to the observed onset of crystallization and its difference from the observed onset of melting, which is a very different phenomenon.

Crystallization. As the theory states, a polymer will crystallize at each and every temperature less than T_m^0. The question is not "will this polymer crystallize at this temperature?" but rather "how long will it take for this polymer to crystallize?" Crystallization comprises both nucleation and growth. Depending on the chosen undercooling, the rate of crystallization will be governed by either the system's ability to nucleate (if closer to T_m^0) or the available energy in the system for chains to move into place and grow existing crystals (if closer to T_g). The rate of crystallization follows a parabolic curve and reaches its maximum somewhere between T_g and T_m^0. Therefore, changes in temperature close to the maximum rate of crystallization have a smaller impact on rate of crystallization than temperature changes closer to the extremes of T_g and T_m^0. It is common to measure crystallization halftime (i.e., the time to reach 50% crystallized at a given temperature by DSC) as the overall rate of crystallization. Alternatively, crystallization rate can be determined by monitoring the spherulitic growth rate from laser light scattering or polarized optical microscopy.

Relationship between crystallization and arresting diffusive motion (physical gelation). It is important to note that while segments of chains are incorporated into stable crystalline regions, the entire chain is not necessarily included in the crystal. Real crystals generally are observed to follow either adjacent re-entry or switchboard models of chain-folded lamella instead of extended chain arrangements. As regions of crystallinity develop in a polymer, they restrict the mobility of the pieces of polymer chains remaining in the amorphous bulk, thus increasing the viscosity. It is also important to note that a polymer may not be "100 % crystalline" when it is deemed "100 % crystalized." A polymer may be considered highly crystalline with 40-60 % v/v regions of crystallinity. The key attribute is that due to the long chain nature of common thermoplastic polymers, the viscosity has become prohibitively high for long-range diffusive motion to occur, thus kinetically preventing molecules from reaching the crystal front. In this way, it is possible and likely to have different absolute values of crystalline content (vol. %) at the "50 % crystallized" point in time to determine crystallization halftime.

The relationship between crystallization and viscosity results in the phenomenon known as physical gelation. At this critical volume fraction of crystalline regions, the polymer behaves like a gel and long-range molecular motion is arrested. The point of physical gelation has been measured in literature using dynamic mechanical analysis (DMA). Using DMA, one can determine the temperature where measured tan(δ) is independent of frequency, such as reported by Hirayama, et al. [18]. This temperature is taken as T_{gel} and can be mapped to a critical percent crystallinity through DSC using the matching rate of cooling.

Roadmap

According to Google Scholar, the article in which the following quote appears has been cited 1636 times at the date of this manuscript.

> "As the molten polymer cools down below T_m, polymer crystals nucleate and grow, recreating regions of ordered molecular chains (crystallites) mixed up with disordered amorphous regions...However, the freezing of the polymer at T_m coincides with an important shrinkage (phenomenon not occurring with amorphous polymers), that may induce geometrical inaccuracies and distortion of the part. A good way to prevent this is to preheat the polymer powder to a temperature slightly below its melting temperature and keep it there for a certain time after consolidation. [19]"

This is a good example of the dangers of imprecise language. So long as one understands "melting temperature" in the quoted text to mean "equilibrium melting temperature (T_m^0)," there is no issue. But if one incorrectly assumed "T_m" to be the peak melting temperature observed from a dynamic DSC experiment, that person would have an incorrect understanding of the physics governing PBF/LB-P.

This example misconception is one the authors aim to remedy or at least raise awareness. For the remainder of the manuscript, the authors discuss additional experimental methods that more thoroughly capture the interplay between temperature, viscosity, and crystallization in the PBF/LB context than the "sintering window." This includes reporting the equilibrium melting temperature, crystallization halftimes, and physical gelation for two commercially available nylon-12 powders marketed for PBF/LB and a generic nylon-12 control. For the sake of clarity, the authors use the distinguishing language "polymeric material" when referring to total material

formulations including not only the base polymer but also processing aids and additives typical of commercial materials.

Materials and Methods

Two commercially available nylon-12 powders were studied for this work. Duraform 2200 is a common nylon-12 powder that is white in color sold for use with CO_2 laser systems ($\lambda = 10.6\ \mu m$). Sintratec PA12 is a black nylon12 powder sold for use with shorter wavelength laser systems (e.g., λ = 1065 nm, 440 nm). A nylon-12 pellet-form sample purchased from Sigma Aldrich was chosen as a "non-AM grade" control material. This pellet is optically clear and does not contain additional compounds for any particular form of manufacturing.

Differential scanning calorimetry (DSC) was performed using a Mettler Toledo DSC 3+. All samples were run by typical heat-cool-heat experimental method at 10 °C min^{-1}. These were combined with thermogravimetric analysis (TGA) experiments on a Mettler Toledo TGA 2 at 10 °C min^{-1} to construct the typical "SLS sintering window." These experiments were conducted under nitrogen atmospheres.

Isothermal crystallization experiments were carried out on the same DSC 3+ to determine equilibrium melt behavior. Samples were heated above 200 °C for 10 min before quenching to the isothermal temperature and holding for 130 min. The Sigma Pellet and DF2200 samples were held at 166, 164, 162, 160, and 158 °C whereas the Sintratec PA-12 material was held at 161, 160, 159, 158, and 157 °C to obtain suitable data.

Physical gelation experiments were conducted on a Mettler Toledo DMA/SDTA 1+ using liquid nitrogen cooling and a special shear fixture designed for low viscosity samples. Samples were prepared by melting raw material (powder or pellets) into an approximately 1.5 mm thick rectangle to ensure a homogeneous sample during testing. These rectangles were loaded into the DMA at room temperature. Samples were held in the melt state at 200 °C for 5 min before cooling at 1 °C min^{-1} to 130 °C. Modulus and phase angle were collected simultaneously using a frequency series of 1, 5, 10, 100, and 150 Hz. The Mettler Toledo DMA/SDTA 1+ switches between operating in a stress- or strain-controlled manner. The limits of 30 N force amplitude and 100 μm displacement amplitude were set in the method. One cycle is defined by satisfying a logical "OR" condition of either the force amplitude *or* displacement amplitude. Samples were observed to satisfy the 100 μm displacement condition before reaching 30 N over the entire range of temperatures tested.

Results and Discussion

Observed Melting and Equilibrium Melting

Distinguishing between "observed melting behavior" and the "intrinsic equilibrium melting temperature" is critical for understanding how semicrystalline polymers behave during thermal processing. When discussing the Process Window, it is often said that the powder bed surface temperature is set slightly below the onset of melting [15]. The more precise statement is that it is set just below the *observed* onset of melting of the powdered feedstock. This observed onset of melting is not intrinsic to a given polymer, but rather is a manifestation of a specific material formulation previously processed at a set of conditions to elicit a chosen morphology. Material formulation, which includes not only the chemical identity, molecular weight, and

molecular weight distribution of the base polymer (e.g., polyamide-12) but also the various commercial "processing aids" (e.g., viscosity modifiers and crystallization packages) and "value adding fillers" (e.g., colorants and reinforcing fibers), affects both the observed and equilibrium melting behavior as different formulations can influence the type of crystalline order (i.e., a different lattice structure or inter-chain spacing). Figure 2 shows the extrapolation from a linear fit of plotting peak melting temperature against isothermal crystallization temperature for DF2200 (white nylon-12), Sintratec PA12 (black nylon-12), and a nylon-12 pellet from Sigma Aldrich used as a non-AM grade control. The intersection from linear extrapolation and the line where $T_m = T_c$ is taken to be T_m^0 by the Hoffman-Weeks approach. The calculated spread of equilibrium melting temperatures is nearly 7 °C with the pellet control presenting the highest equilibrium melting temperature.

The basic definition of equilibrium melting temperature is the theoretical melting temperature for a perfect extended chain crystal [16]; it is therefore independent of processing conditions. Both observed and equilibrium melting behavior are important for understanding how a given polymeric material behaves during PBF/LB. Equilibrium melting temperature is key to understand for mapping the overall possible process parameter space while observed melting behavior helps to contextualize a specific instance of prior processing. For example, the observed melting behavior of nylon-12 [20] and poly(phenylene sulfide) [21] change with repeated processing; however this will not affect T_m^0 as prior processing does not alter fundamental crystal structure. Processing any given material formulation imparts a specific morphology, which includes crystal size, crystal size distribution, and the crystal-to-amorphous ratio. These factors may greatly influence the observed melting behavior without altering T_m^0. The shifting of melt behavior between the first and second heats in a typical heat-cool-heat DSC experiment is one example of altering semi-crystalline morphology within a polymer without altering the equilibrium melting behavior.

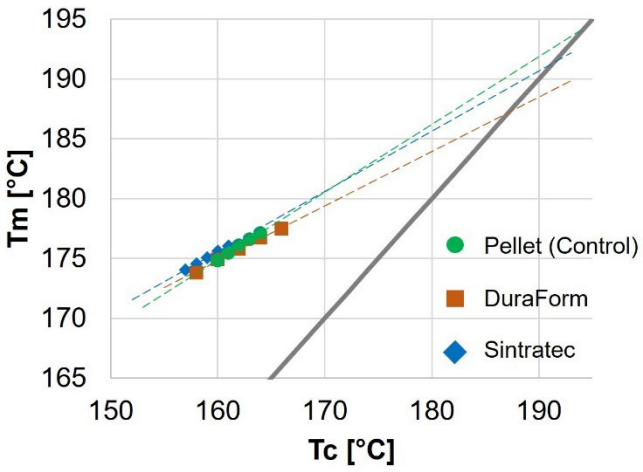

Figure 2: Equilibrium melting temperature determination using Hoffman-Weeks approach for two commercially available "PBF/LB grade" nylon-12 polymers and generic nylon-12 pellet control. Equilibrium melting temperature is calculated to be 194.3 °C for the control pellet, 191.3 °C for Sintratec PA12, and 187.2 °C for DF2200.

Onset of melting observed in the first heat of a DSC experiment is apt and suitable for determining the absolute upper-bound for bed temperature, as this experiment adequately captures the morphology induced by the powder making process (for virgin powder) or the morphology induced by repeated use in PBF/LB.

Table 1: Tabulated Results from DSC

	Tm, onset	Tm, endset	Tm, peak	Hm	Tc, onset
Sample	[°C]	[°C]	[°C]	[J g-1]	[°C]
DF2200	171.7	181.3	171.6	21.2	147.7
Sintratec PA12	173.1	180.1	177.7	24.6	157.4
Sigma Pellet (Control)	162.8	182.9	177.7	51.9	152.8

Work from Zarringhalam, et al. highlighted the core/shell partial melting phenomenon they observed following PBF/LB printing of nylon-12 [22]. This sort of behavior is expected if the entire particle does not reach the equilibrium melt temperature; only above T_m^0 will all crystalline order surely be erased. Therefore, the authors suggest T_m^0 and not simply $T_{m,end}$ as the more ideal minimum threshold temperature resulting from laser scanning.

Crystallization Kinetics

Given that the equilibrium melting temperature is the threshold below which crystallizable polymers will crystallize, the next question becomes "how long will it take to crystallize?" Predominant work mathematically describing the nucleation and growth of polymer crystallization was published by Lauritzen and Hoffman [17] and Avrami [23]. Many researchers use Equation 1 from Lauritzen and Hoffman or Equation 2 from Avrami as the starting point for studying a particular polymeric material in a particular processing context. Either isothermal (Lauritzen-Hoffman) or non-isothermal (Avrami) experiments can be conducted and fit to these equations for extrapolating beyond tested conditions or feeding predictive models.

$$W_c = C \cdot exp\left[\frac{-U^*}{R\,(T_c - T)}\right] \cdot exp\left[\frac{-K_g}{T_c\,(T_m^0 - T_c)}\right] \tag{1}$$

$$X_c\,(t) = 1 - exp(-Kt^n) \tag{2}$$

Figure 3 depicts the measured crystallization halftimes and mathematically fit data for the two PBF/LB nylon-12 powders and pellet control material. The figure focuses on the temperature region of interest for typical PBF/LB bed temperatures; however, the full shape of the data is a "U" nestled between T_g and T_m^0. Given the known difficulties in maintaining a constant, consistent temperature across the entire build area [24], understanding the sensitivity of a polymeric material's crystallization kinetics around the chosen temperature range is critical to affect desired performance properties and avoid out-of-plane warping. As shown in the figure, crystallization halftimes can vary over 100 minutes in the typical range for bed temperatures between 170-165 °C.

Interestingly, for a technology concerned with ensuring a slow crystallization to maximize particle coalescence and minimize out-of-plane warping, the "PBF-grade" materials have a shorter crystallization half-time than the control pellet at 160 °C. The fit of Sintratec PA12 data to the Lauritzen-Hoffman equation indicates a short crystallization half-time even out to 175 °C. This is unsurprising given the known presence of filler material included for short-wave laser absorption that can act as a heterogenous nucleating agent. The industrial, white material DF2200 tracks closer to the control pellet. Based on Figure 3, the typical bed temperatures for printing nylon12, and potential build times of more than 12 h (720 min), one must conclude that it is unlikely for the entire part to "remain molten" for the entire build. Zhao, et al. report that, at minimum, the lower layers will begin to crystallize during PBF/LB based on their measured crystallization kinetics, which is reported as a deviation to what is commonly understood for the process [26]. Even considering that subsequent scanning of the laser re-heats and (at least partially) re-melts crystalline domains in a chosen layer of interest, Chatham, et al. report that around 430 s (7.17 min) is the last time the temperature of a chosen layer of interest rises above the onset of melting for the laser parameter combination with highest energy tested [27]. Their work mapping cyclic thermal profiles measured during printing tensile specimens to crystallization kinetics indicates that useful molecular diffusion for coalescence is arrested due to crystallization after 500 - 600 s (8.34 - 10 min).

Recall from the Introduction that the patent literature stated the magnitude of separation between observed crystallization and melting behavior in a dynamic DSC experiment was a good indicator of crystallization kinetics; slower crystallization kinetics would be accompanied by a larger separation between the two peaks. The presented data runs counter to this statement. The order of decreasing crystallization halftimes at 170 °C is (1) Sigma Aldrich control pellet, (2) DF2200, then (3) Sintratec PA12. Therefore, one would expect the same ranked order for decreasing degree

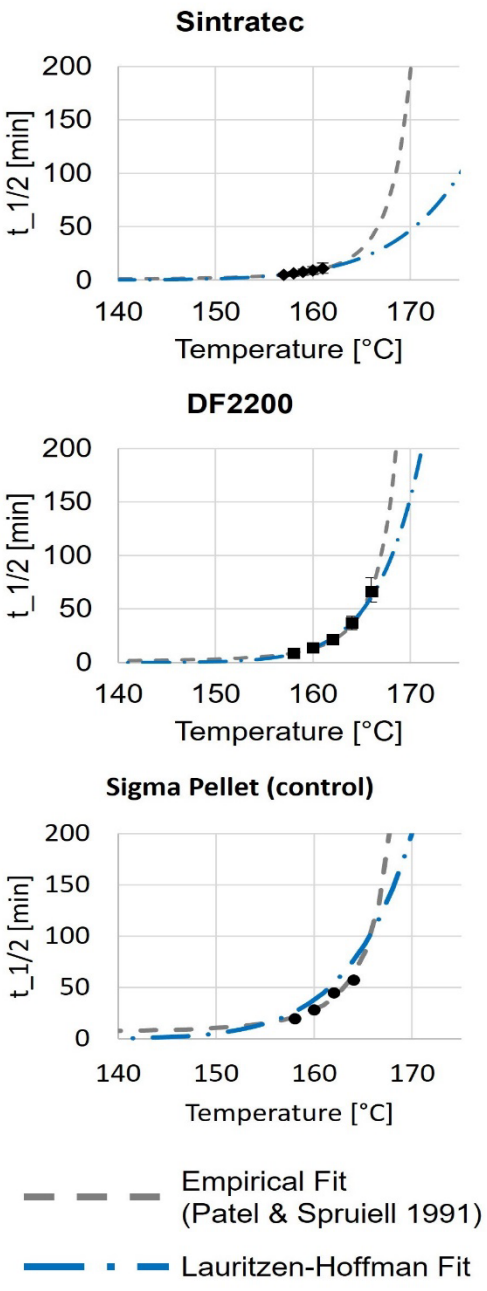

Figure 3: Time to reach 50% crystallized at indicated isothermal temperatures for DF2200, Sintratec PA12, and the Sigma Aldrich nylon-12 control pellet. Data were fit to both the original Lauritzen-Hoffman equation (dot-dash) [17] and an empirical version published by Patel and Spruiell (dashed line) [25].

of melt/crystallization peak separation, but instead the Sigma Aldrich control pellet has the smallest extent of separation between peaks (See Figure 1). This underscores the importance of thorough consideration based in experimentation when considering new materials for PBF/LB.

Physical Gelation

Experiments in the previous sections focus on the energetics of crystallization measured via DSC. By contrast, physical gelation is measured via DMA as the mechanical response to crystallization. Molecular ordering into crystalline domains significantly increases a material's modulus above T_g. While this process begins at local, discrete nucleation sites, subsequent growth of crystalline domains results in a gel-like network structure with the domains acting as physical crosslinks. The temperature at which this behavior begins can be determined via the frequency independent tan(δ); that is, the intersection of tan(δ) curves collected at multiple frequencies. The results from such an experiment are presented in Figure 4. The gelation temperature can be subsequently related to DSC experimentation at the same cooling rate to determine the extent of crystallization at the gelation temperature. When additionally combined with crystallization halftime data, candidate materials can be evaluated based on calculated time available for fusion, such as in Chatham, et al. [27].

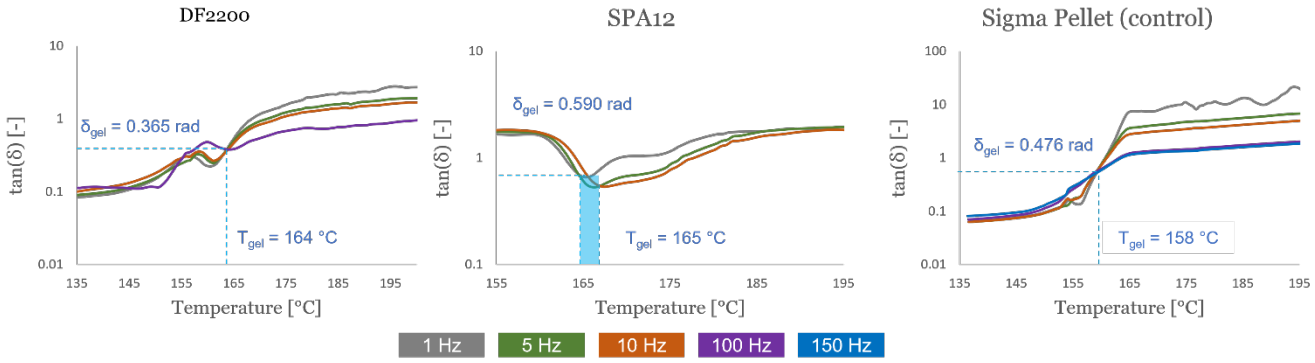

Figure 4: tan(δ) collected at various frequencies plotted against temperature as the samples cool and crystallize from the melt state. The frequency independent junction of all curves is considered to be the physical gelation point.

In addition to temperature for gelation, the retardation angle (δ_{gel}) is reported in Figure 4. This angle relates to the power law exponent n for typical mathematical representation of polymer complex modulus ($G*$) in the following manner: $\delta_{gel} = \frac{n\pi}{2}$. The retardation angle is also related to the stiffness S of the gel. Correlations between gel stiffness and warping should be the subject of future work.

It should be noted that while the control PA12 pellet material from Sigma Aldrich presents a textbook example of frequency-independent tan(δ), the two samples of "PBF grade" powder show a wider range of crossover behavior smearing the gelation temperature. This is perhaps due to the complex nature of the fully formulated powder, which likely includes flow agents in addition to laser absorbers and crystallization controlling compounds. These additional components may prevent true frequency independence from occurring and may also introduce a deviation from power-law type behavior for the complex modulus. However, the crossover spread remains in a tight temperature window of less than 3 °C, which is on the order of reliable temperature control for typical PBF systems.

Proposed New Processing Window

In light of the discussed understanding of polymer crystallization, the authors propose the following revisions to the "PBF/LB-P Processing Window" from the common diagram based on vague patent language:

- Use $T_m{}^0$ for target minimum threshold temperature for laser scanning.
- Use T_{gel} obtained through DMA to determine the threshold for cooling and the critical percent crystallinity.
- Use $t_{1/2}$ and in situ $T(t)$ profiles to estimate the time to reach critical percent crystallinity.

These revisions are combined into Figure 5 for the DF2200 (white) and Sintratec PA12 (black) PBF/LB powders in addition to the Sigma Aldrich nylon-12 pellet control.

The composite figure includes more and more relevant information summarizing polymer melting, crystallization, and degradation behavior than traditionally included when discussing polymers in the PBF/LB manufacturing context. The overlaid data simply summarizes polymer behavior, but additional interpretation is needed to translate the results into the PBF/LB manufacturing context. Certain aspects are true physical thresholds, like the equilibrium melting temperature; however, many aspects are time-dependent and kinetic effects must be carefully considered when choosing process parameter settings.

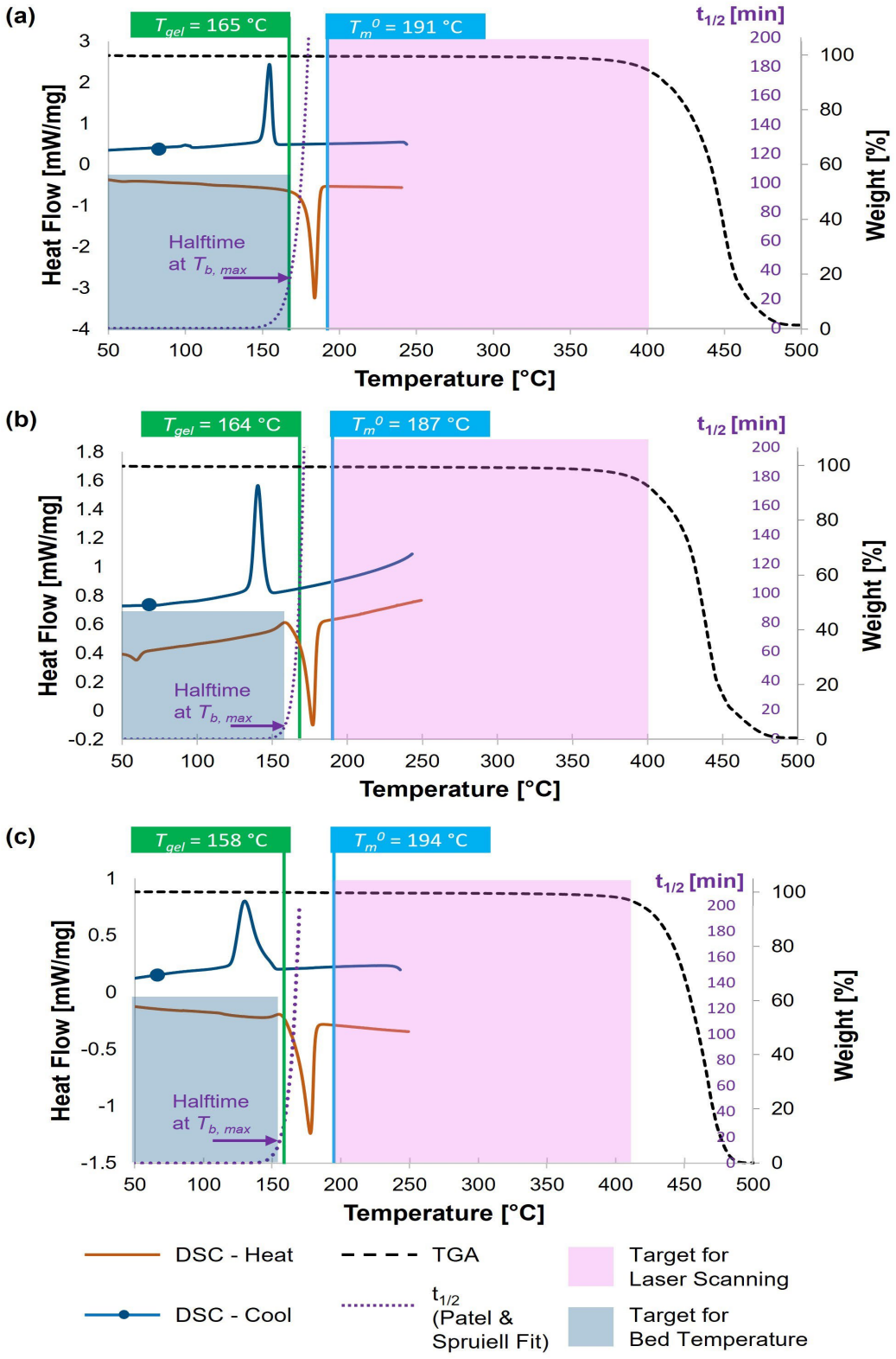

Figure 5: Proposed new "PBF/LB-P Processing Window" diagrams for (a) Sintratec PA12 (black) powder, (b) DF2200 (white) powder, and (c) Sigma Aldrich nylon-12 pellet control. Diagram comprises DSC first heating and cooling, TGA, crystallization half-time, equilibrium melting temperature, and physical gelation temperature.

Note that the observed onset of melting is less than (or very close to) T_{gel} for all materials studied. Therefore, the T_b must be set below T_{gel}, which certainly allows for physical gelation to occur during printing. Given the goal of prolonging the coexistence of the recently-laser scanned melt with the solid-never-melted surrounding powder, the arrow indicating crystallization halftime at maximum bed temperature is a key metric to consider. Even though the Sintratec PA12 powder has the fastest crystallization rate at any given temperature of the three materials studied, its combination with the higher observed onset of melting enables successful printing. Similarly, the lower T_{gel} of the Sigma control pellet contributes to a prolonged time available for fusion; this is especially true if ensuring the temperature of the scanned region reaches above T_m^0 increasing total ΔT. In many ways, the difference between T_m^0 and T_{gel} is the scientifically more rigorous version of what was originally desired through the "SLS process window" looking at the observed onsets of melting and crystallization from the dynamic DSC experiment. Framing polymer crystallization during PBF/LB around equilibrium melting and physical gelation is more consistent with established polymer science literature, which helps promote a correct understanding of polymer response to process stimuli truly enabling data-driven decision making when synthesizing novel materials or adapting and formulating existing materials for PBF/LB.

The presented example new composite figure for nylon-12 does not significantly differ from the typical diagram created based on the original patent language. This should be expected given that nylon-12 has been the dominant material studied and commercialized based on those patents. The authors expect material behavior for materials beyond nylon-12 to more significantly differ between the more rigorous "new window" diagram and typical window. It will, perhaps, explain the ability to print PEK HP3 and PPS despite not following the traditional separation of melting and crystallization window as reported in the literature [28, 29]. It should also be noted that the proposed new window diagram still does not include a direct representation of warping or the "50 μm out of plane threshold" suggested by the DTM patents [11, 12]. This should be the focus of future work, even though this behavior will likely show a heavy dependence on the geometry of the specific toolpath for the given layer than a true material property.

Conclusions

Interdisciplinary teams are becoming more and more commonplace as society looks to tackle larger, more complex and interconnected issues. Such collaboration is only possible with a common vocabulary. This manuscript highlighted several terms pertaining to the melting and crystallization phenomena of polymers in the PBF/LB context that have historically imprecise meanings leading to misconceptions of the governing physics of this AM process. The authors hypothesize that this language and terminology barrier is hindering development, adaption, and commercialization of PBF/LB-P as the misunderstandings may result in research teams dismissing polymers outright for not having a "wide sintering window" instead of pressing in to determine suitable processing conditions.

The authors summarize the key concepts of equilibrium melting temperature, isothermal crystallization, non-isothermal crystallization, and physical gelation as they have been well-studied in polymer science and briefly connect these topics to PBF/LB. Figure 5 graphically demonstrates the interplay of these phenomena and the authors briefly discussed how to use this figure to choose process parameters. The authors hope that these topics will be more thoroughly explored in the context of many new polymers being considered for PBF/LB applications.

References

[1] J. Beaman, D. L. Bourell, C. Seepersad, D. Kovar, Additive manufacturing review: Early past to current practice, Journal of Manufacturing Science and Engineering 142 (11) (2020).

[2] A. Mokrane, M. Boutaous, S. Xin, Numerical analysis of the heating phase and densification mechanism in polymers selective laser melting process, in: AIP Conference Proceedings, Vol. 1960, AIP Publishing LLC, 2018, p. 140013.

[3] R. G. Kleijnen, M. Schmid, K. Wegener, Production and processing of a spherical polybutylene terephthalate powder for laser sintering, Applied Sciences 9 (7) (2019) 1308.

[4] M. Schmid, R. Kleijnen, M. Vetterli, K. Wegener, Influence of the origin of polyamide 12 powder on the laser sintering process and laser sintered parts, Applied Sciences 7 (5) (2017) 462.

[5] Y. Khalil, N. Hopkinson, A. J. Kowalski, J. P. A. Fairclough, Investigating the feasibility of processing activated carbon/uhmwpe polymer composite using laser powder bed fusion, Polymers 14 (16) (2022). doi:10.3390/polym14163320. URL https://www.mdpi.com/2073-4360/14/16/3320

[6] D. Drummer, D. Rietzel, F. Kühnlein, Development of a characterization approach for the sintering behavior of new thermoplastics for selective laser sintering, Physics Procedia 5 (2010) 533–542.

[7] D. Drummer, K. Wudy, F. Kühnlein, M. Drexler, Polymer blends for selective laser sintering: material and process requirements, Physics Procedia 39 (2012) 509–517.

[8] S. Greiner, K. Wudy, L. Lanzl, D. Drummer, Selective laser sintering of polymer blends: Bulk properties and processbehavior, Polymer Testing64 (2017) 136–144. doi:https://doi.org/10.1016/j.polymertesting.2017.09.039.

URL
https://www.sciencedirect.com/science/article/pii/S0142941817309170

[9] ASTM/ISO 52900 - additive manufacturing - general principles - terminology (2021).

[10] C. R. Deckard, Method and apparatus for producing parts by selective sintering, uS Patent 4,863,538 (Sep. 5 1989).

[11] E. D. Dickens Jr, B. L. Lee, G. A. Taylor, A. J. Magistro, H. Ng, Sinterable semi-crystalline powder and near-fully dense article formed therewith, US Patent 5,342,919 (Aug. 30 1994).

[12] E. D. Dickens Jr, B. L. Lee, G. A. Taylor, A. J. Magistro, H. Ng, K. P. McAlea, P. F. Forderhase, Sinterable semi-crystalline powder and near fully dense article formed therein, US Patent 5,648,450 (Jul. 15 1997).

[13] G. Wang, P. Wang, Z. Zhen, W. Zhang, J. Ji, Preparation of pa12 microspheres with tunable morphology and size for use in sls processing, Materials & Design 87 (2015) 656–662.

[14] E. D. Bain, Polymer powder bed fusion additive manufacturing: Recent developments in materials, processes, and applications, Polymer-Based Additive Manufacturing: Recent Developments (2019) 7–36.

[15] C. A. Chatham, T. E. Long, C. B. Williams, A review of the process physics and material screening methods for polymer powder bed fusion additive manufacturing, Progress in Polymer Science 93 (2019) 68–95. doi:10.1016/j.progpolymsci.2019.03.003.

[16] P. C. Painter, M. M. Coleman, Essentials of polymer science and engineering, DEStech Publications, Inc, 2008.

[17] J. D. Hoffman, J. J. Weeks, Melting process and the equilibrium melting temperature of polychlorotrifluoroethylene, J. Res. Natl. Bur. Stand., Sect. A 66 (1) (1962) 13–28.

[18] T. Hirayama, T. Uneyama, Y. Masubuchi, Characterization of critical gel state of polyamides by viscoelastic, thermal, and ir measurements, Rheologica Acta 58 (2019) 281–290.

[19] J.-P. Kruth, G. Levy, F. Klocke, T. Childs, Consolidation phenomena in laser and powder-bed based layered manufacturing, CIRP annals 56 (2) (2007) 730–759.

[20] S. Dadbakhsh, L. Verbelen, O. Verkinderen, D. Strobbe, P. Van Puyvelde, J.-P. Kruth, Effect of pa12 powder reuse on coalescence behaviour and microstructure of sls parts, European Polymer Journal 92 (2017) 250–262.

[21] C. A. Chatham, A. Das, T. E. Long, M. J. Bortner, C. B. Williams, Ageing of pbf-grade poly(phenylene sulfide) powder and its effect on critical printability properties, Macromolecular Materials and Engineering 306 (3) (2021). doi:10.1002/mame.202000599.

[22] H. Zarringhalam, C. Majewski, N. Hopkinson, Degree of particle melt in nylon-12 selective laser-sintered parts, Rapid Prototyping Journal (2009).

[23] M. Avrami, Granulation, phase change, and microstructure kinetics of phase change. iii, The Journal of chemical physics 9 (2) (1941) 177–184.

[24] S. Fish, J. C. Booth, S. T. Kubiak, W. W. Wroe, A. D. Bryant, D. R. Moser, J. J. Beaman, Design and subsystem development of a high temperature selective laser sintering machine for enhanced process monitoring and control, Additive Manufacturing 5 (2015) 60–67.

[25] R. M. Patel, J. E. Spruiell, Crystallization kinetics during polymer processing—analysis of available approaches for process modeling, Polymer Engineering & Science 31 (10) (1991) 730–738.

[26] M. Zhao, K. Wudy, D. Drummer, Crystallization kinetics of polyamide 12 during selective laser sintering, Polymers 10 (2) (2018) 168.

[27] C. A. Chatham, M. J. Bortner, B. N. Johnson, T. E. Long, C. B. Williams, Predicting mechanical property plateau in laser polymer powder bed fusion additive manufacturing via the critical coalescence ratio, Materials & Design 201 (2021). doi:10.1016/j.matdes.2021.109474.

[28] S. Berretta, K. Evans, O. Ghita, Predicting processing parameters in high temperature laser sintering (ht-ls) from powder properties, Materials & Design 105 (2016) 301–314.

[29] C. A. Chatham, T. E. Long, C. B. Williams, Powder bed fusion of poly(phenylene sulfide) at bed temperatures significantly below melting, Additive Manufacturing 28 (2019) 506–516. doi:10.1016/j.addma.2019.05.025.